

Matter-enhanced spin-flavor precession of solar neutrinos with transition magnetic moments

A. B. Balantekin, P. J. Hatchell, and F. Loreti

Physics Department, University of Wisconsin, Madison, Wisconsin 53706

(Received 31 January 1990; revised manuscript received 7 March 1990)

Experimental and astrophysical limits on the neutrino magnetic moments and the magnetic fields in the solar interior are briefly reviewed. For the case of simultaneous flavor mixing and nonzero transition magnetic moments left-handed electron-neutrino survival probability contours are calculated for Cl and Ga detectors for several possible magnetic-field configurations. A possible explanation of the variation of the solar-neutrino flux with the solar cycle is pointed out. This solution requires a magnetic field in the bottom of the convective zone of the Sun with $B \sim (1-2) \times 10^5$ G and a transition magnetic moment of $(5-10) \times 10^{-12} \mu_B$.

I. INTRODUCTION

After it was experimentally determined¹ that the measured solar-neutrino capture rate on Earth is about one-third of the standard solar-model prediction,² neutrino oscillations were proposed as a possible mechanism to resolve the discrepancy between experiment and theory. One recently proposed solution to the problem of missing solar neutrinos is the Mikheyev-Smirnov-Wolfenstein (MSW) effect.^{3,4} In this scenario coherent forward scattering of neutrinos in electronic matter can cause an almost complete conversion of electron neutrinos to neutrinos of a different flavor. This effect does not require a fine-tuning of mixing angles and mass differences; hence it provides a possible solution to the solar-neutrino problem within the current theoretical prejudices. The elegance and the utility of the MSW effect has been demonstrated in the existing literature.^{5,6}

If the neutrinos have large magnetic moments there exists a more speculative solution to the solar-neutrino problem: transmission through the solar magnetic field may flip the neutrinos' spin, changing the left-handed electron neutrino into a right-handed neutrino⁷ that is not detectable by the existing nuclear (i.e., ³⁷Cl) detectors. More recently it has been observed that there might possibly be an anticorrelation between the sunspot number and the capture rate of solar neutrinos.⁸ Motivated by this observation, Okun, Voloshin, and Vysotsky⁹ elaborated on this scenario, noting that, in addition to the electric or magnetic dipole moments, it is also conceivable to have flavor transition moments between different species. Akhmedov¹⁰ and Barbieri and Fiorentini¹¹ investigated further the effects of matter on the resonant amplification of the flavor-changing neutrino spin rotation. After a careful analysis of the current situation, Bethe¹² concluded that this anticorrelation can probably not be ascribed to the matter fluctuations in the convective zone of the Sun caused by localized magnetic fields.

The combined effect of matter and magnetic fields on neutrino spin and flavor precession was examined by Lim and Marciano.¹³ They pointed out that the simultaneous presence of flavor mixing and magnetic (diagonal or transition) moments can give rise to two new resonances in

addition to the MSW one. This possibility was studied by Minakata and Nunokawa¹⁴ who concluded that one needs a rather large magnetic field and/or magnetic moment for an emphatic effect.

In this paper we wish to calculate iso-SNU (solar-neutrino units) figures for the case of simultaneous flavor mixing and nonzero magnetic moments in order to critically examine the conclusions of Refs. 12-14. Our analysis goes beyond that given by Minakata and Nunokawa,¹⁴ who did not investigate the capture rates on various detectors. In Sec. II we discuss experimental and astrophysical limits on the neutrino magnetic moments and the magnetic fields in the solar interior. Equations governing the neutrino propagation when both flavor and chiral components mix are given in Sec. III. We discuss the numerical solution of those equations to obtain iso-SNU curves in Sec. IV. Section V contains a discussion of our results and conclusions.

II. LIMITS ON THE NEUTRINO MAGNETIC MOMENTS AND THE SOLAR MAGNETIC FIELD

A. Magnetic fields in the solar interior

Some of the earlier attempts to solve the solar-neutrino problem invoked the possibility of very large magnetic fields in the interior of the Sun.¹⁵ A very large magnetic field which decreases toward the surface would increase the pressure gradient. To have a significant effect on the calculated neutrino fluxes the magnetic field should be strong enough that $B^2/8\pi$ is a few percent of the gas pressure, which requires a magnetic field of approximately 10^8-10^9 G. Such a large magnetic contribution to the pressure is a large deviation from the standard solar model where the hydrostatic equilibrium is achieved through the gas pressure gradient.¹⁶ Furthermore such an intense field is not expected to persist over the lifetime of the Sun.¹⁷ It is probably safe to assume that any magnetic field in the interior of the Sun which exceeds the value 10^7 G would be in contradiction with the standard solar model. Existing observations¹⁸ of the depth and latitude dependence of solar rotation also set an upper limit of this magnitude [$\sim (0.8-2.0) \times 10^7$ G].

One has a better idea about the magnetic fields in the convective zone and at the surface of the Sun.¹⁹ The convective zone, which is about $0.3R_\odot$ thick, has a large toroidal magnetic field larger than 10^2 – 10^4 G. This field changes its direction every 11 years. The period of 1986–1987 was with minimal solar activity and a small toroidal magnetic field. The previous period of solar activity was 1978–1982 with a magnetic field of $\sim 10^3$ G near the surface. Davis and collaborators (Cl experiment) reported a capture rate of ~ 4.2 SNU in 1977 and ~ 5.0 SNU in 1986–1987 and, more recently, a smaller value.⁸

It further seems to be possible to link density variations at the bottom of the convective zone to the solar activity.²⁰ There is an observed anticorrelation between the solar radius R_\odot with the 11-yr cycle of solar activity, i.e., overall radius of the quiet Sun is larger than that of active Sun. The effect is small: $\sim \Delta R_\odot / R_\odot \approx 10^{-3}$. A plausible scenerio was suggested by Schatzman and Ribes.²⁰ They conjecture that in the quiet Sun a large magnetic field is embedded in the bottom of the convective zone in “ropes” (force tubes) with a radius of about 30 km. If the field strength is $\geq 10^6$ G, then it is strong enough to expel most of the matter from the ropes (magnetic pressure being almost equal to the gas pressure), causing the solar radius to be larger by the observed amount. They consequently speculate that in the quiet Sun there is about 600 km of space near the bottom of the convective zone, where the matter density is very small. In the active Sun, the ropes reach to the surface of the Sun, the density at the bottom of the convective zone increases, and the solar radius decreases.

Endal, Sofia, and Twigg,²¹ using a full hydrostatic stellar-evolution code, examined further the perturbative connection between the displacement of matter inside the convection zone with the displacement of the surface radius. They found out that the radial length of the internal region where the matter is excluded is only about 1% of the change in solar radius. Baltz and Weneser²² presented a heuristic model with essentially the same conclusion. Their arguments lead to

$$d \leq 4 \times 10^{-6} R_\odot$$

for the size of the excluded region. To achieve such a total exclusion at the bottom of the convective zone requires a very large magnetic field of about $\sim 10^8$ G in the gap. However, as these authors point out, the perturbations employed in those models are simplifications of the actual physical mechanisms taking place in the Sun, the dynamics of which is essentially nonperturbative.

B. Neutrino magnetic moments

A simple extension of the minimal standard electroweak model permits massive Dirac neutrinos to acquire finite magnetic dipole moments through radiative corrections.²³ For the electron neutrino one gets

$$|\mu_{\nu_e}| = \frac{3eG_F}{8\sqrt{2}\pi^2} m_{\nu_e} \approx 3.2 \times 10^{-19} \mu_B \left[\frac{m_{\nu_e}}{1 \text{ eV}} \right], \quad (1)$$

where μ_B is the Bohr magneton

$$\mu_B = \frac{e\hbar}{2m_e c} \approx 5.8 \times 10^{-15} \text{ MeV G}^{-1}.$$

The value of the magnetic moment given in Eq. (1) is nonzero, but too small to be astrophysically significant. Introduction of additional physics, such as right-handed currents²⁴ or a charged Higgs extension of the minimal electroweak model,²⁵ could lead to much larger magnetic moments. Supersymmetric²⁶ and superstring-inspired²⁷ models naturally incorporate the latter possibility. A number of models yield not only diagonal magnetic moments but also off-diagonal (transition) moments which can transform left-handed neutrinos of one flavor into the right-handed neutrinos of another flavor in an external transverse magnetic field. Only Dirac neutrinos can have diagonal magnetic moments. Transition magnetic moments are permissible for both Majorana²⁸ and Dirac neutrinos.

Direct experimental bounds on the magnetic moments are rather weak. Antineutrino electron scattering data yield²⁹ a bound of

$$|\mu_{\nu_e}| \leq 4 \times 10^{-10} \mu_B.$$

Astrophysical and cosmological arguments are more restrictive. Stellar cooling (energy loss due to neutrino pair emission) provides³⁰ a bound of

$$|\mu_{\nu_e}| \leq 1 \times 10^{-11} \mu_B.$$

The observation of neutrinos from Supernova 1987A would also restrict the magnetic moments. Lattimer and Cooperstein³¹ and Barbieri and Mohapatra³² considered the emission of right-handed neutrinos after the bounce. By imposing a bound on the luminosity of right-handed neutrinos, they get a limit of

$$|\mu_{\nu_e}| \leq 10^{-13} \mu_B.$$

Nötzold³³ considered the emission during the core collapse (before the bounce) and obtained a limit of

$$|\mu_{\nu_e}| \leq 2 \times 10^{-12} \mu_B.$$

Validity of such limits from supernova was however questioned.³⁴ The first two bounds apply to both Majorana and Dirac moments (diagonal and transition), whereas the supernova bounds apply to Dirac moments. For Dirac neutrinos there is an additional cosmological bound as well. The synthesis of ${}^4\text{He}$ in the big bang would be disrupted by the excitation of additional neutrino helicity states unless³⁵

$$|\mu_{\nu_e}| \leq 2 \times 10^{-11} \mu_B.$$

This bound does not apply to the Majorana-neutrino transition moments, since for Majorana neutrinos no extra degrees of freedom are excited. A good summary of the current situation together with a list of possible terrestrial experiments that might observe a magnetic moment was given by Vogel and Engel.³⁶

III. SPIN-FLAVOR PRECESSION IN MATTER

A. Evolution of chiral components

For the electron neutrino the chiral components ν_{eL} and ν_{eR} interact differently with matter. This difference tends to suppress precession by splitting their degeneracy. The equation describing the propagation through matter of the two helicity components of a Dirac neutrino with mass m_ν and magnetic moment $\mu_{e\nu}$ is^{9–11}

$$i \frac{d}{dt} \begin{pmatrix} \nu_{eL} \\ \nu_{eR} \end{pmatrix} = \begin{pmatrix} a_e(t) & \mu B \\ \mu B & -a_e(t) \frac{m_\nu^2}{2p^2} \end{pmatrix} \begin{pmatrix} \nu_{eL} \\ \nu_{eR} \end{pmatrix}, \quad (2)$$

where B is the transverse magnetic field and a_e is the contribution of matter to the effective mass. In the standard model (for an unpolarized neutral medium) one gets

$$a_e(t) = \frac{G_F}{\sqrt{2}} (2N_e - N_n), \quad (3)$$

where N_e and N_n are electron and neutron number densities, respectively. In the limit $m_\nu/p \rightarrow 0$, which we consider hereafter, the right-handed neutrino does not interact with matter.

Writing the magnetic moment in terms of Bohr magnetons,

$$\mu = g \mu_B, \quad (4)$$

where g is a small number, it is possible to calculate the survival probability of the left-handed component (in moderate magnetic fields) using the logarithmic perturbation theory following Ref. 6 where the same method was applied to the MSW effect. For the survival probability at time T we find

$$P(\nu_{eL} \rightarrow \nu_{eL}) = \exp \left[-g^2 \mu_B^2 \left| \int_0^T dt B(t) e^{iQ_e(t)} \right|^2 + O(g^4) \right], \quad (5)$$

where

$$Q_e(t) = \frac{G_F}{\sqrt{2}} \int_0^t dt (2N_e - N_n). \quad (6)$$

The resonance condition is $N_e = N_n/2$. It is unlikely to achieve this resonance condition in the Sun where the neutron density is $N_n \approx N_e/6 \sim N_e/3$. It can however be achieved in a supernova.^{34,37}

B. Spin-flavor precession in the Sun

In this case we consider two generations. The neutrino evolution equation is^{13,14}

$$i \frac{d}{dt} \begin{pmatrix} \nu_{eL} \\ \nu_{\mu L} \\ \nu_{eR} \\ \nu_{\mu R} \end{pmatrix} = \begin{pmatrix} H_L & BM^\dagger \\ BM & H_R \end{pmatrix} \begin{pmatrix} \nu_{eL} \\ \nu_{\mu L} \\ \nu_{eR} \\ \nu_{\mu R} \end{pmatrix}, \quad (7a)$$

where the 2×2 submatrices are

$$H_L = \begin{pmatrix} \frac{\Delta m^2}{2E} \sin^2 \theta + a_e & \frac{\Delta m^2}{4E} \sin 2\theta \\ \frac{\Delta m^2}{4E} \sin 2\theta & \frac{\Delta m^2}{2E} \cos^2 \theta + a_\mu \end{pmatrix}, \quad (7b)$$

$$M = \begin{pmatrix} \mu_{ee} & \mu_{e\mu} \\ \mu_{\mu e} & \mu_{\mu\mu} \end{pmatrix}, \quad (7c)$$

and $H_R = H_L(a_e = 0 = a_\mu)$. In the above equations θ is the mixing angle, Δm^2 is the difference of the squares of the masses, and E is the neutrino energy. For a neutral, unpolarized medium, the matter potentials are

$$a_e = \frac{G_F}{\sqrt{2}} (2N_e - N_n), \quad a_\mu = -\frac{G_F}{\sqrt{2}} N_n. \quad (8)$$

Note that we assume the right-handed components ν_{eR} and $\nu_{\mu R}$ mix in the same way as the left-handed components do as it was assumed in Ref. 14. This is different than the convention in Ref. 13, where the right-handed components are taken to be the same as vacuum mass eigenstates.

There are four possible crossing resonances. The

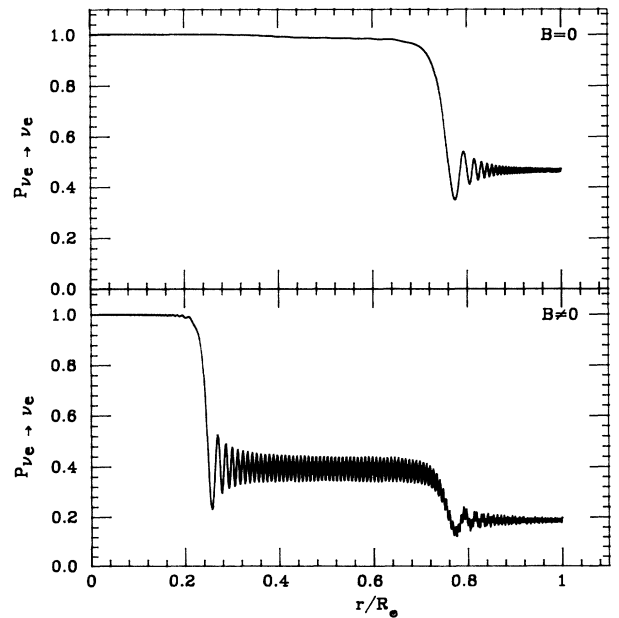


FIG. 1. A comparison of the MSW and the $\nu_{eL} \rightarrow \nu_{\mu R}$ resonances as discussed in the text. The upper panel (where $B=0$) exhibits only the MSW resonance and the lower panel (where $B \neq 0$) exhibits both resonances for the same electron density distribution (see text). In the Sun these two resonances coalesce.

$\nu_{e_L} \rightarrow \nu_{e_R}$ resonance discussed in the previous subsection:

$$\frac{G_F}{\sqrt{2}}(2N_e - N_n) = 0; \quad (9a)$$

the MSW resonance

$$\sqrt{2}G_F N_e = \frac{\Delta m^2}{2E} \cos 2\theta; \quad (9b)$$

the $\nu_{e_L} \rightarrow \nu_{\mu_R}$ resonance

$$\frac{G_F}{\sqrt{2}}(2N_e - N_n) = \frac{\Delta m^2}{2E} \cos 2\theta; \quad (9c)$$

and the $\nu_{\mu_L} \rightarrow \nu_{e_R}$ resonance

$$\frac{G_F}{\sqrt{2}} N_n = \frac{\Delta m^2}{2E} \cos 2\theta. \quad (9d)$$

For the Sun, where the neutron density is only about 20% of the electron density, the MSW and the $\nu_{e_L} \rightarrow \nu_{\mu_R}$ resonances are very close to each other. In fact they become almost a single resonance.¹⁴ On the other hand, for a supernova, where the neutron density changes very rapidly during the collapse, the $\nu_{e_L} \rightarrow \nu_{e_R}$ resonance (which is due to a diagonal magnetic moment) and the $\nu_{e_L} \rightarrow \nu_{\mu_R}$ resonance (which is due to a transition magnetic moment) are very close to each other, especially for the large ener-

gies that one expects the supernova neutrinos to carry (note that Δm^2 is also expected to be quite small). This feature makes it rather difficult to put separate limits on diagonal and transition magnetic moments using the supernova data.

To compare the MSW and the $\nu_{e_L} \rightarrow \nu_{\mu_R}$ resonances we present a rather distorted situation in Fig. 1, where we used an artificial matter density and rather large (~ 20 kG) magnetic field for the purpose of separating the resonances. In this figure the electron density is taken to be $50 \text{ cm}^{-3}/N_A$ at $r/R_\odot = 0$, where N_A is Avogadro's number. It has a Wood-Saxon shape and levels off to $40 \text{ cm}^{-3}/N_A$ at $r/R_\odot = 0.3$. It then remains approximately constant until $r/R_\odot = 0.6$ where another Wood-Saxon function takes it to $33 \text{ cm}^{-3}/N_A$ at $r/R_\odot = 1$. The magnetic resonance was selected to occur at an electron density $43 \text{ cm}^{-3}/N_A$, chosen to be at $r/R_\odot = 0.25$, and the MSW resonance at an electron density $\sim 39.5 \text{ cm}^{-3}/N_A$ at $r/R_\odot = 0.75$. The separation of the resonances in this figure is due to our choice of the density (the flatness of the region inbetween). As was discussed above, they do not separate in the Sun for a wide range of parameters. We illustrated that to separate them requires a rather drastic change in the solar electron density.

In the case of Majorana neutrinos, it is not possible to have a diagonal magnetic moment and the Hamiltonian takes the form

$$H_{\text{Maj}} = \begin{pmatrix} a_e & \frac{\Delta m^2}{4E} \sin 2\theta & 0 & \mu^* B \\ \frac{\Delta m^2}{4E} \sin 2\theta & \frac{\Delta m^2}{2E} \cos 2\theta + a_\mu & -\mu^* B & 0 \\ 0 & -\mu B & -a_e & \frac{\Delta m^2}{4E} \sin 2\theta \\ \mu B & 0 & \frac{\Delta m^2}{4E} \sin 2\theta & \frac{\Delta m^2}{2E} \cos 2\theta - a_\mu \end{pmatrix}. \quad (10)$$

IV. NUMERICAL ANALYSIS

In our calculations all densities, fluxes, and cross sections are in accord with the standard solar model and were taken from Bahcall.¹⁶ We have assumed that the magnetic field is either nonzero throughout the entire Sun or localized in a particular region (i.e., throughout the convective zone). In the former case the magnetic field profile was taken to be a Wood-Saxon shape of the form

$$B(r) = \frac{B_0}{1 + \exp[10(r - R_\odot)/R_\odot]}, \quad (11)$$

where B_0 is the strength of the magnetic field at the center of the Sun. In the latter case we take the magnetic field confined to the convective zone of the Sun as we will discuss in the next section. We also take the diagonal magnetic moments to be zero, since for the solar neutron

density they cannot induce a resonant transition [cf. the discussion following Eqs. (9)]. Note that in Eq. (7), which describes the motion of a neutrino through the Sun, the transition magnetic moment and the magnetic field appear only in the combination $\mu_{e\mu} B$.

The numerical calculation was performed by diagonalizing the Hamiltonian numerically in the dimensionless variable $\rho = (\Delta m^2/E)r$:

$$H(\rho) = S(\rho)D(\rho)S^T(\rho), \quad (12)$$

where S and S^T are the orthogonal diagonalization matrices, and D is the diagonal matrix of the eigenvalues. Since, for a sufficiently small step size, the density and the magnetic field vary slowly with ρ , the ρ dependence of the Hamiltonian in each step can be neglected giving

$$\Psi(\rho + \Delta\rho) = S e^{-iD\Delta\rho} S^T \Psi(\rho) \quad (13)$$

as the algorithm for calculating Ψ from one step to the next. Here Ψ is the column vector in Eq. (7a). The radial dependence of the flux of neutrinos from each reaction was taken into account by stepping backward from the edge of the magnetic field toward the center of the Sun. The probabilities are first averaged over distance in the vacuum giving

$$\bar{P}_{ie} = (1 - \frac{1}{2}\sin^2 2\theta)P_{ie}(\rho_{\text{edge}}) + \frac{1}{2}\sin^2 2\theta P_{i\mu}(\rho_{\text{edge}}) - \sin 2\theta \cos 2\theta \text{Re}[v_{ie}(\rho_{\text{edge}})v_{i\mu}(\rho_{\text{edge}})], \quad (14)$$

where $P_i(\rho_{\text{edge}})$ and $v_i(\rho_{\text{edge}})$ are the probability and the amplitude, respectively, that an electron neutrino which started life at ρ_i has become, at the edge of the magnetic field, an electron neutrino or a muon neutrino. The averaged probability at the edge of the magnetic field for the left-handed electron neutrinos from reaction j is then

$$\bar{P}_e^j \left[\frac{\Delta m^2}{E}, \sin^2 2\theta, \rho_{\text{edge}} \right] = \sum_i \phi^j(\rho_i) \bar{P}_{ie} \left[\frac{\Delta m^2}{E}, \sin^2 2\theta, \rho_{\text{edge}} \right], \quad (15)$$

where $\phi^j(\rho_i)$ is the fraction of electron neutrinos of type j produced at ρ_i .

The probabilities for the iso-SNU contour plots are obtained by averaging over neutrino energy for a fixed mass difference and mixing angle:

$$P(\Delta m^2, \sin^2 2\theta) = \frac{\sum_j \int dE \sigma(E) \Phi_j(E) \bar{P}_e^j(\Delta m^2, E, \sin^2 2\theta)}{\sum_j \int dE \sigma(E) \Phi_j(E)}, \quad (16)$$

where $\sigma(E)$ is the cross section for a given detector at energy E , and $\Phi_j(E)$ is the flux at energy E of neutrinos from reaction j . Since the probabilities are a function of the ratio of mass difference to energy, the probabilities as a function of energy were obtained by fixing θ and Δm^2 such that $P(\Delta m^2/E, \theta) = P(\Delta m^2, E, \theta)$.

V. DISCUSSION AND CONCLUSIONS

In Figs. 2 and 3 we plot the left-handed electron neutrino survival probability contours, in the parameter space of Δm^2 and $\sin^2 2\theta$, for the Cl and Ga detectors, respectively. In calculating these contours we assumed that the magnetic field extends over the entire Sun and used the profile in Eq. (11). For each figure, $\mu_{e\mu} B_0$ is taken to be (a) 0.0, (b) 2.0×10^{-7} , (c) 5.0×10^{-7} , and (d) $10.0 \times 10^{-7} \mu_B$ G. The survival probability contours plotted range from 0.1 (the dotted line), to 0.9 (the dashed line), with a step size of 0.1.

An examination of Figs. 2 and 3 reveals that introduction of a magnetic field and a transition magnetic moment can alter the iso-SNU plots rather substantially. Comparing the $B=0$ case with $B \neq 0$ cases, we see that for large values of Δm^2 ($\geq 10^{-5}$ eV²) and small values of the mixing angle, solar magnetic field plays no role. The

reason for this is the relative locations of the MSW and the $\nu_{eL} \rightarrow \nu_{\mu R}$ resonances in the Sun. The latter resonance occurs at a higher density than the former [cf. Eqs. (9b) and (9c)]. For large Δm^2 and small θ , even the central density of the Sun is not large enough for the $\nu_{eL} \rightarrow \nu_{\mu R}$ resonance to occur. Hence in this region of the

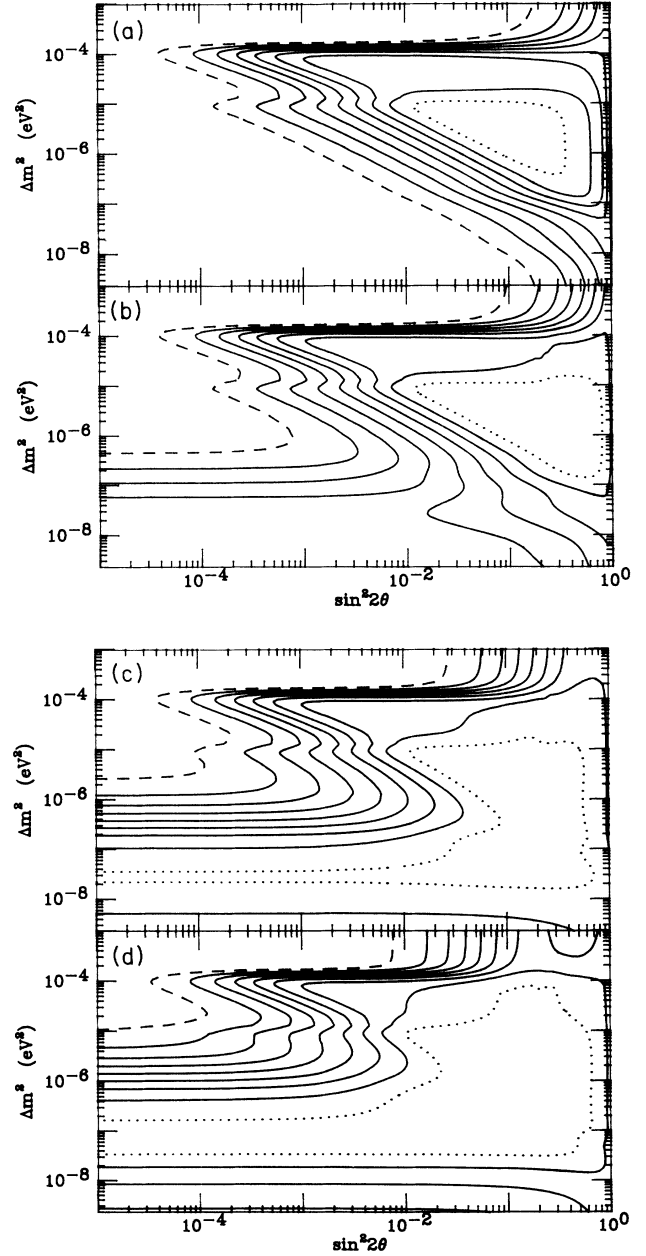


FIG. 2. Left-handed electron Dirac-neutrino survival probability contours for the Cl detector based on the standard solar model as given in Ref. 16. The magnetic field is assumed to extend over the entire Sun with the profile given in Eq. (11) of the text. The diagonal neutrino magnetic moments are taken to be zero (the transition magnetic moment being nonzero). The contours range from 0.1 (the dotted line) to 0.9 (the dashed line) in successive steps of 0.1. (a) $\mu B = 0$, (b) $\mu B = 2 \times 10^{-7} \mu_B$ G, (c) $\mu B = 5 \times 10^{-7} \mu_B$ G, (d) $\mu B = 10 \times 10^{-7} \mu_B$ G.

parameter space the iso-SNU plot is unchanged.

The behavior for small θ and small values of Δm^2 ($\leq 10^{-5}$ eV²) is intriguing. One observes that the iso-SNU contours are independent of the mixing angle. In this region the $\nu_{eL} \rightarrow \nu_{\mu R}$ resonance can take place in the

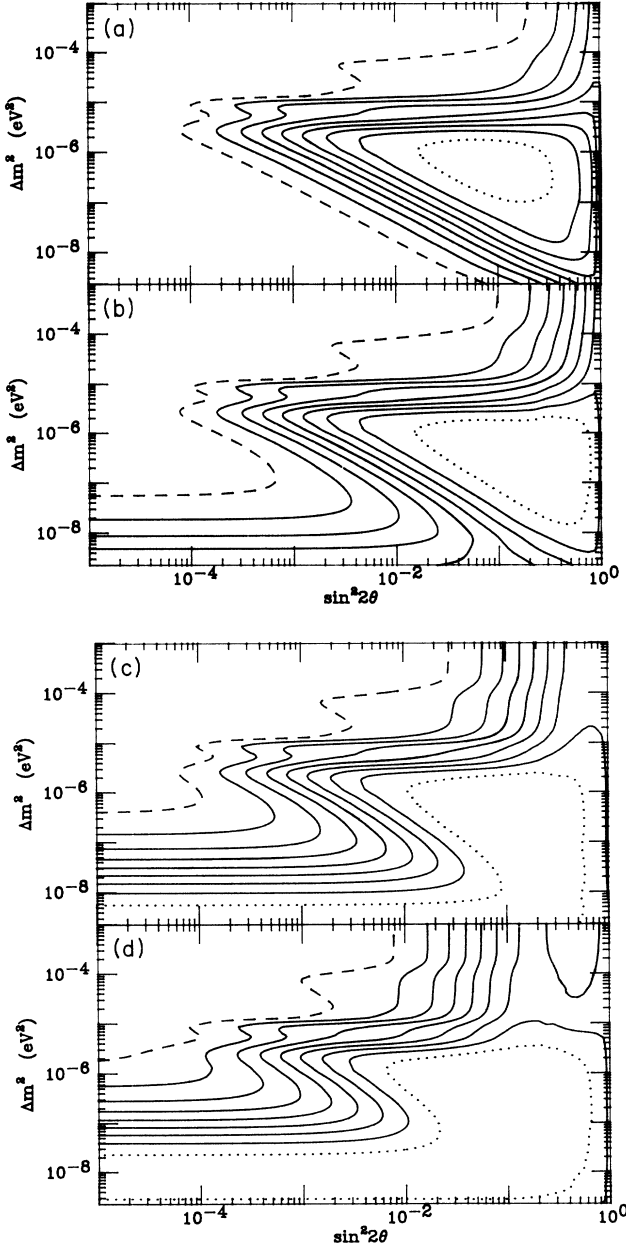


FIG. 3. Left-handed electron Dirac-neutrino survival probability contours for the Ga detector based on the standard solar model as given in Ref. 16. The magnetic field is assumed to extend over the entire Sun with the profile given in Eq. (11) of the text. The diagonal neutrino magnetic moments are taken to be zero (the transition magnetic moment being nonzero). The contours range from 0.1 (the dotted line) to 0.9 (the dashed line) in successive steps of 0.1. (a) $\mu B = 0$, (b) $\mu B = 2 \times 10^{-7} \mu_B$ G, (c) $\mu B = 5 \times 10^{-7} \mu_B$ G, (d) $\mu B = 10 \times 10^{-7} \mu_B$ G.

Sun, and, as Δm^2 decreases, its location moves from the center of the Sun to the surface. Equation (9c) implies that for a given value of E there is a value of Δm^2 which places the $\nu_{eL} \rightarrow \nu_{\mu R}$ resonance at the center of the Sun. The lower E is the lower this Δm^2 will be. Since the Ga detector is sensitive to lower neutrino energies than the Cl detector, for the former the value of Δm^2 which corresponds to the central density is lower. Indeed, in our plots, this region is shifted to smaller values of Δm^2 for the Ga detector.

For each detector, there are two features of this region (small θ) of the plots which can be noted. The first concerns the variation of the contour lines, as Δm^2 is decreased, for a fixed value μB . The second concerns the variation in the contour lines as μB is changed for a fixed value of Δm^2 . In the first case, one sees that as Δm^2 is decreased the probability drops to a minimum value and then rises again as Δm^2 is decreased further [cf. Figs. 2(d) and 3(d)]. In the second case one sees that as μB is increased the probability, after reaching a minimum, re-bounds to larger values. For example, for $\Delta m^2 \sim 2 \times 10^{-8}$ eV², the probability is 0.1 for $\mu B_0 = 5 \times 10^{-7} \mu_B$ G and 0.2 for $\mu B_0 = 10 \times 10^{-7} \mu_B$ G. Both of these features can be understood by considering only the 2×2 submatrix for ν_{eL} conversion into $\nu_{\mu R}$, since the MSW resonance is essentially absent in this region, a fact which we also verified numerically. We write

$$i \frac{d}{dt} \begin{pmatrix} \nu_{eL} \\ \nu_{\mu R} \end{pmatrix} = \frac{1}{2} \begin{pmatrix} a_e(t) - \frac{\Delta m^2}{2E} \cos 2\theta & 2\mu B \\ 2\mu B & -a_e(t) + \frac{\Delta m^2}{2E} \cos 2\theta \end{pmatrix} \times \begin{pmatrix} \nu_{eL} \\ \nu_{\mu R} \end{pmatrix}, \quad (17)$$

where everything is defined as in Sec. III B and B is taken to be a constant over the resonance region. The crucial point to note is that in this case the width of the resonance region is given by

$$\delta r = \left| \frac{1}{2N_e - N_n} \frac{d(2N_e - N_n)}{dr} \right|^{-1} \frac{4\mu BE}{\Delta m^2 \cos 2\theta}. \quad (18)$$

Using the approximate electron density given by Bahcall,¹⁶

$$N_e(r) = 245 \exp(-10.54r/R_\odot) N_A \text{ cm}^{-3}, \quad (19)$$

and assuming $N_n \sim N_e/6$, one can rewrite the width of the resonance in terms of the solar radius:

$$\delta r = \frac{4\mu BE}{\Delta m^2 \cos 2\theta} \frac{R_\odot}{10.54}. \quad (20)$$

We see that if $\mu B E / \Delta m^2$ gets large, not only does the resonance move toward the edge of the Sun, but also the width of the resonance could be a significant fraction of the solar radius. Therefore, as Δm^2 is decreased beyond a certain value with μB fixed, the survival probability decreases by a smaller amount when the neutrino reaches the edge of the Sun. The same effect occurs if one holds Δm^2 fixed and increases μB . To illustrate this effect, in Fig. 4 we plot the survival probability as a function of the distance from the center of the Sun for a fixed μB [Fig. 4(a)] and for a fixed $\Delta m^2/E$ [Fig. 4(b)]. Note that in Fig. 4(a), decreasing $\Delta m^2/E$, or in Fig. 4(b), increasing μB , gives rise to a larger width and correspondingly a larger survival probability.

For a chlorine detector, there is a jog to smaller θ values at $\Delta m^2 \sim 10^{-5} \text{ eV}^2$ (especially for the survival probabilities ≥ 0.3) for almost all values of the magnetic

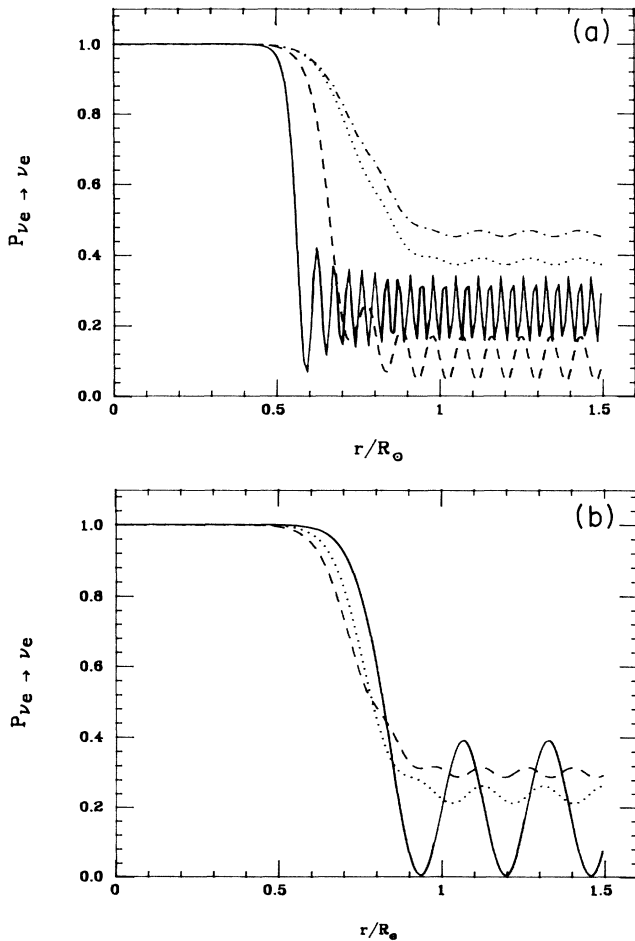


FIG. 4. (a) Left-handed electron-neutrino survival probability as a function of the distance from the center of the Sun for a fixed $\mu B (10^{-6} \mu_B \text{ G})$ for $\Delta m^2/E$ equal to $10^{-7} \text{ eV}^2/\text{MeV}$ (the solid line), $3 \times 10^{-8} \text{ eV}^2/\text{MeV}$ (the dashed line), $6 \times 10^{-9} \text{ eV}^2/\text{MeV}$ (the dotted line), and $2 \times 10^{-9} \text{ eV}^2/\text{MeV}$ (the dashed-dotted line). (b) Left-handed electron-neutrino survival probability as a function of the distance from the center of the Sun for a fixed $\Delta m^2/E (10^{-8} \text{ eV}^2/\text{MeV})$ for μB equal to $4 \times 10^{-7} \mu_B \text{ G}$ (the solid line), $7 \times 10^{-7} \mu_B \text{ G}$ (the dotted line), and $10 \times 10^{-7} \mu_B \text{ G}$ (the dashed line).

field. This effect is due to the monoenergetic (0.862-MeV) neutrinos coming from electron capture on ${}^7\text{Be}$. Although the capture cross section on ${}^{37}\text{Cl}$ is small at this energy, the flux of these neutrinos is large enough that it contributes significantly to the energy averaging in Eq. (16) for larger values of $\Delta m^2/E$. Again for a chlorine detector for $\Delta m^2 \sim 10^{-4} \text{ eV}^2$, the survival probability seems to be independent of the mixing angle. Higher values of Δm^2 do not seem to contribute to the resonances. This can be understood by noting that the maximum flux of ${}^8\text{B}$ neutrinos occurs at $\sim 10 \text{ MeV}$, which corresponds to a MSW resonant density [cf. Eq. (9b)] close the maximum density of the Sun. For larger values of Δm^2 , the ${}^8\text{Be}$ neutrinos do not undergo resonance. Similarly, because of the ${}^7\text{Be}$ line source a false top of the MSW triangle is reached at $\Delta m^2 \sim 10^{-5} \text{ eV}^2$, since the energy of the ${}^7\text{Be}$ neutrinos is approximately a factor of 10 smaller than the energy of the maximum flux of ${}^8\text{B}$.

A comparison of the Dirac and Majorana neutrino survival probabilities is given in Figs. 5 and 6 for the Cl and Ga detectors, respectively. One observes that the plots are very similar except for the large $\sin^2 2\theta$ and large Δm^2 region. It is hard to distinguish between the Dirac and Majorana neutrinos by observing only the left-handed electron neutrino. Being able to detect the neutral current would enable us to distinguish between those two possibilities. The B solar- ν experiment (BOREX) detector, based on the nucleus ${}^{11}\text{B}$, could perform such a task.³⁸ A full analysis, enumerating all the possibilities, of the capture of both neutrinos and antineutrinos on ${}^{11}\text{B}$ will be given elsewhere.³⁹

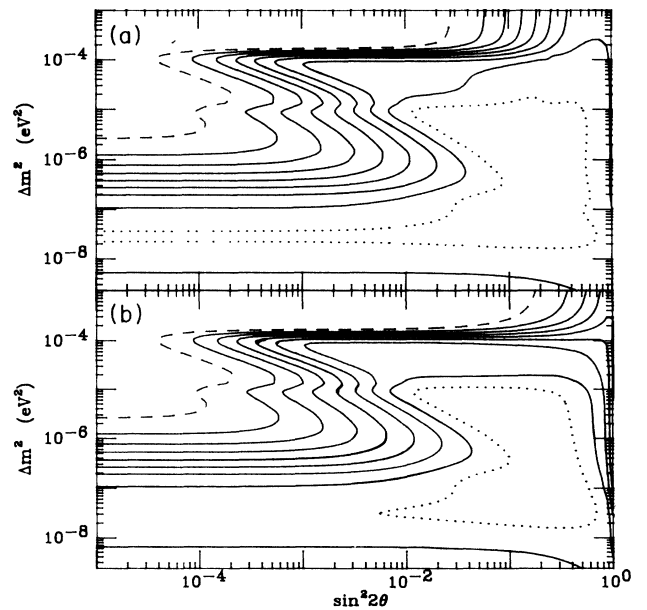


FIG. 5. A comparison of the Dirac (a) and Majorana (b) electron-neutrino survival probabilities for the Cl detector. The contours range from 0.1 (the dotted line) to 0.9 (the dashed line) in successive steps of 0.1. The calculation was done as described in the caption of Fig. 2 using only transition magnetic moments for the Dirac neutrinos. μB is taken to be $5 \times 10^{-7} \mu_B \text{ G}$.

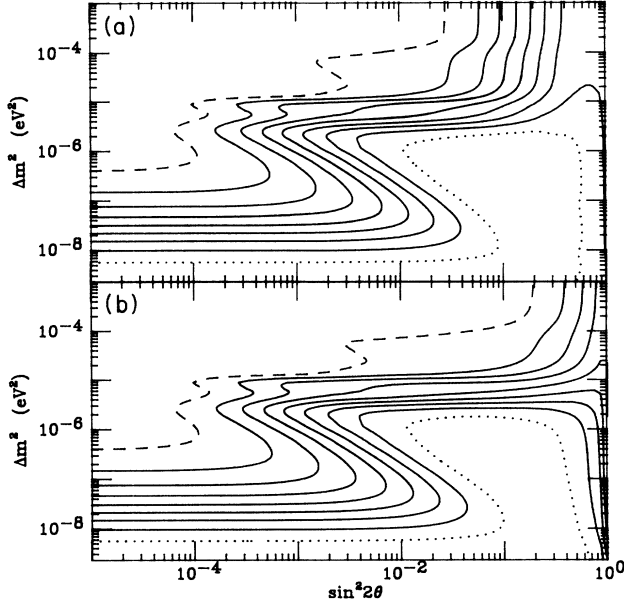


FIG. 6. Same as Fig. 5, but for a Ga detector.

Although it describes the wealth of the possibilities, the magnetic-field profile we have employed so far is not very realistic; it is very large at the surface of the Sun. A more realistic magnetic-field profile for the Sun in its active period was given by Sofia and his collaborators.^{21,40} Following their analysis, we repeated our calculations for

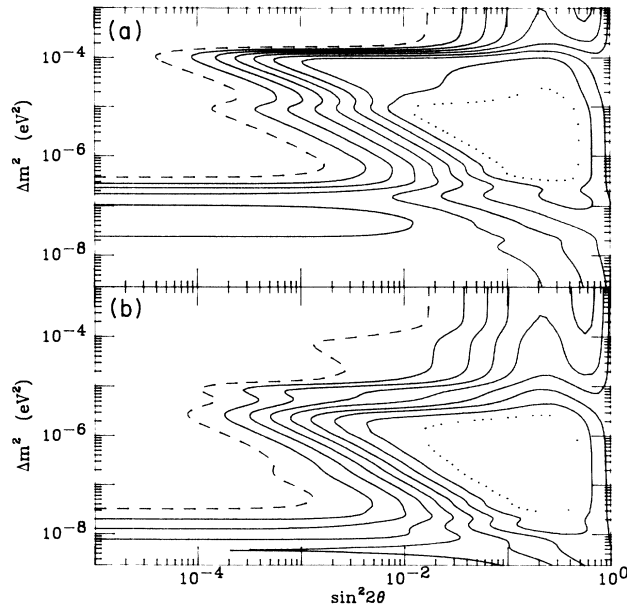


FIG. 7. (a) Left-handed Dirac electron-neutrino survival probability for the Cl detector with the magnetic field localized in the convective zone as described in the text. $\mu_{e\mu}$ is taken to be $10^{-11} \mu_B$. The contours range from 0.1 (the dotted line) to 0.9 (the dashed line) in successive steps of 0.1. (b) The same for the Ga detector.

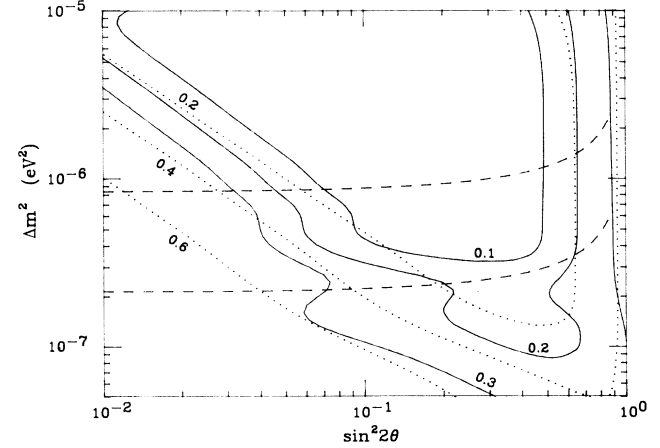


FIG. 8. The comparison of the survival probabilities for the Cl detector in the quiet Sun (the dotted lines) and the active Sun (the solid lines). For the active Sun the magnetic field is confined to the convective zone as calculated by Endal, Sofia, and Twigg (Ref. 21) and the transition magnetic moment is taken to be $10^{-11} \mu_B$. The dotted lines go from a survival probability of 0.2 (the innermost one) to 0.6 (the outer one) in steps of 0.2. The solid lines go from a survival probability of 0.1 (the innermost one) to 0.3 (the outer one) in steps of 0.1. The region below the upper dashed line corresponds to the situation where the location of the $\nu_{eL} \rightarrow \nu_{\mu R}$ resonance is outside $0.52R_\odot$. The region below the lower-dashed line corresponds to the situation where the location of the $\nu_{eL} \rightarrow \nu_{\mu R}$ resonance is outside $0.71R_\odot$.

a magnetic-field spread only over the convective zone of the Sun. This magnetic field changes from zero at $0.7R_\odot$ to 10^5 G at $0.75R_\odot$. It remains constant until $0.8R_\odot$, after which point it falls linearly to 2×10^3 G at the surface of the Sun. Although this value of the surface field is realized only at the sunspots, the contribution of the surface region to the reduction in probability is negligible; hence, the error made is rather small. Such a field is consistent with the observed variations in the solar luminosity and the solar radius.^{21,40} In our calculation the transition magnetic moment was taken to be $10^{-11} \mu_B$. The results are presented in Figs. 7(a) and 7(b) for Cl and Ga detectors, respectively. Such a value of transition magnetic moment would be in contradiction with the supernova bounds and marginally consistent with the astrophysical and cosmological bounds presented in Sec. II B. The validity of supernova bounds were criticized.³⁴ Furthermore it would be prudent to assign at least a factor of 2 uncertainty to the magnetic field inside the Sun leading to a magnetic moment of 5×10^{-12} . (Recall that only the combination μB appears in the Hamiltonian.) Nevertheless a solution of the solar-neutrino problem with Dirac neutrinos carrying transition magnetic moments seems to be only marginally feasible.

There is no consensus about the magnitude and location of the magnetic field in the quiet Sun. It is conceivable that this field leaves the convective zone altogether and moves into the radiative zone during this period. In such a scenario, even if it were to increase by an order of

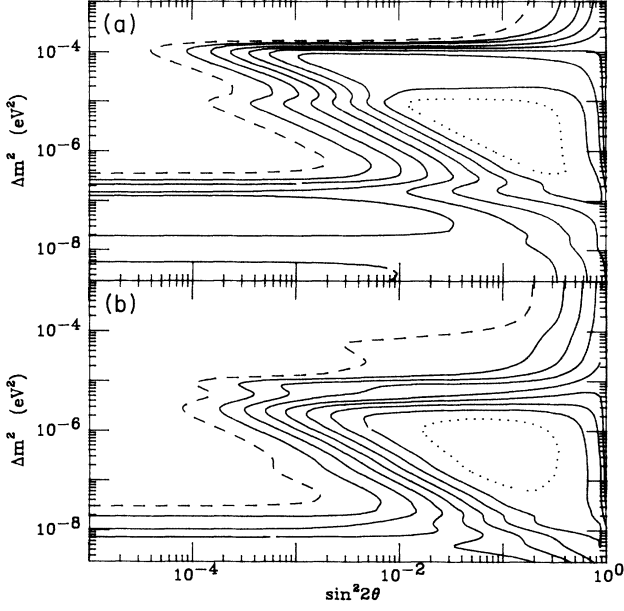


FIG. 9. (a) Majorana electron-neutrino survival probability for the Cl detector with the magnetic field (with a maximum value of 10^5 G) localized in the convective zone as described in the text. μ is taken to be $10^{-11} \mu_B$. The contours range from 0.1 (the dotted line) to 0.9 (the dashed line) in successive steps of 0.1 (b) The same for the Ga detector.

magnitude and were confined to a very small region, its percentage contribution to the pressure, hence its effect on the matter density, would be negligible. The location of the $\nu_{e_L} \rightarrow \nu_{\mu_R}$ resonance is given by the value of the solar density, which satisfies the condition exhibited in Eq. (9c). For sufficiently small values of Δm^2 , the position of this resonance is located in the upper radiation zone or the convective zone. If there is no magnetic field present at this location then a resonant conversion of the ν_{e_L} into ν_{μ_R} will not occur. We assume that in the quiet Sun this is the case and the neutrinos go through only the MSW resonance. As can be seen in Fig. 8, this choice results in the anticorrelation of the neutrino flux with the solar cycle. In this figure the survival probabilities of the left-handed electron neutrino for the quiet Sun (the dotted lines) and the active Sun (the solid lines) are compared for a Cl detector. The dotted lines go from a survival probability of 0.2 (the innermost one) to 0.6 (the outer one) in steps of 0.2. The solid lines go from a survival probability of 0.1 (the innermost one) to 0.3 (the outer one) in steps of 0.1. One observes that for the values of $\sin^2 2\theta$ around 0.1, the solar-neutrino flux is reduced by a factor of 2 in the active Sun as compared to the quiet Sun. The dashed lines indicate the region of the parameter space where the assumptions mentioned above are realized. The region below the upper-dashed line corresponds to the situation where the location of the $\nu_{e_L} \rightarrow \nu_{\mu_R}$ resonance is outside $0.52R_\odot$ (i.e., the magnetic field should lie inside this radius in the quiet Sun). The region below the lower-dashed line corresponds to the situation where the location of the $\nu_{e_L} \rightarrow \nu_{\mu_R}$ resonance is outside $0.71R_\odot$.

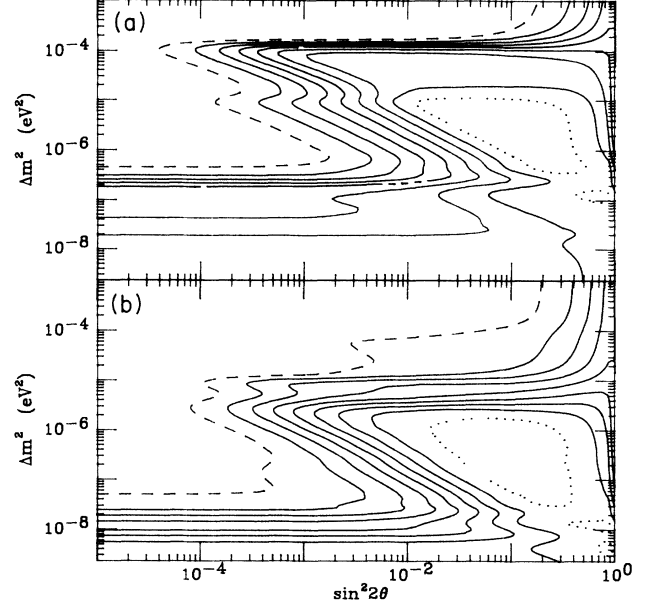


FIG. 10. (a) Majorana electron neutrino probability for the Cl detector with the magnetic field (with a maximum value of 2×10^5 G) localized in the convective zone as described in the text. μ is taken to be $10^{-11} \mu_B$. The contours range from 0.1 (the dotted line) to 0.9 (the dashed line) in successive steps of 0.1. (b) The same for the Ga detector.

Another, independent, test of this explanation to the anticorrelation of the neutrino flux with the solar activity will be possible when the data from the Ga detectors are available. One observes that the values of Δm^2 and $\sin^2 2\theta$, which give rise to the reduction by a factor of 2 in the Cl detector, also yield a very small counting rate during the solar activity at the Ga detector: A survival probability of ~ 0.1 or a capture rate of ~ 12 SNU. Furthermore, this capture rate varies by much less than a factor of 2 during the solar cycle. If the observed capture rate for Ga turns out to be much larger than this value, other alternatives should be investigated.

As we discussed in Sec. II B the supernova bounds and the cosmological bound from the He synthesis in the early Universe do not apply to the case of Majorana neutrinos. Hence a solution of the solar-neutrino problem with Majorana neutrinos carrying magnetic moments is perhaps more viable. In Figs. 9(a) and 9(b), the survival probability contours for the Majorana neutrinos are shown for Cl and Ga detectors, respectively. In calculating these probabilities we used the more realistic magnetic-field profile of Sofia and collaborators^{21,40} discussed above and a transition magnetic moment of $10^{-11} \mu_B$. If the magnetic field were larger by a factor of 2, then it would instead mean a magnetic moment of $5 \times 10^{-12} \mu_B$. Indeed it is this range of values of μB where one starts observing significant changes in the iso-SNU plot for mass differences below 10^{-6} eV^2 . To illustrate this change we show the survival probability contours in Figs. 10(a) (Cl) and 10(b) (Ga) for the value of the magnetic field twice that used in Fig. 9. From Figs. 9 and 10, one observes that there is a region of the param-

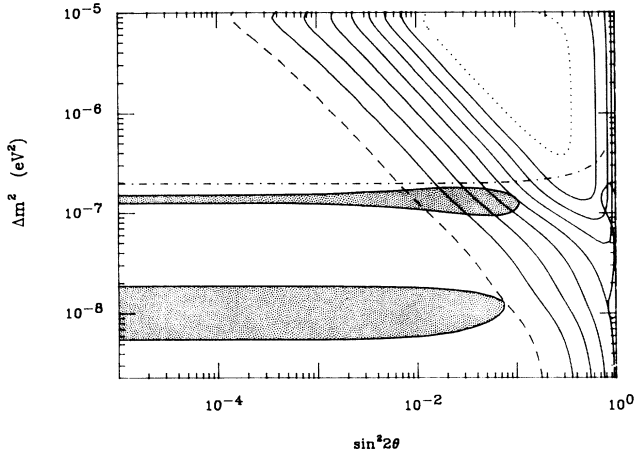


FIG. 11. The comparison of the survival probabilities for the CI detector in the quiet and active Sun. The contours are the survival probabilities for the quiet Sun ($B=0$) and the shaded area represents the region where a reduction of 40% or more can be achieved in the active Sun. In the active Sun the magnetic field is confined to the convective zone as calculated by Endal, Sofia, and Twigg (Ref. 21) (with a maximum value of 10^5 G). The transition magnetic moment is taken to be $10^{-11} \mu_B$. The region below the dotted-dashed line corresponds to the situation where the location of the $\nu_e \rightarrow \bar{\nu}_\mu$ resonance is outside $0.7R_\odot$.

ter space where the survival probabilities vary by a factor of approximately 2 as compared to the $B=0$ case. We exhibit this region in Figs. 11 and 12. In Fig. 11, the contours represent the survival probabilities with no magnetic field (i.e., quiet Sun). The shaded areas show the regions of the parameter space where the survival probabilities are reduced by 40% or more when the magnetic field (with a maximum value of 10^5 G used in Fig. 9) is introduced. We again assume that the magnetic field leaves the convective zone and the neutrinos go through only the MSW resonance in the quiet Sun. The region below the dotted-dashed line in Fig. 11 corresponds to the situation where the location of the $\nu_e \rightarrow \bar{\nu}_\mu$ resonance is outside $0.7R_\odot$. One observes that for the values of $\sin^2 2\theta$ around 0.1 and Δm^2 around 10^{-7} eV², the solar-neutrino flux is reduced by an amount of 40% or more in the active Sun as compared to the quiet Sun. A similar calculation is presented in Fig. 12 for the magnetic field with a maximum value of 2×10^5 G used in Fig. 10. The shaded region in Fig. 12 represents the region of the parameter space where the survival probabilities are reduced by an amount of 50% or more in the active Sun as compared to the quiet Sun. In this case all of the parameter space below $\Delta m^2 \sim 10^{-7}$ eV² can be used to achieve a reduction of by a factor of 2 or more. Note that [cf. Figs. 9(b) and 10(b)] for the region of the parameter space which could account for the anticorrelation of the solar-neutrino flux with the solar cycle, the Ga count rate is still small.

In this paper we presented survival probability contours for the solar electron neutrinos for the case of simultaneous flavor mixing and nonzero transition mag-

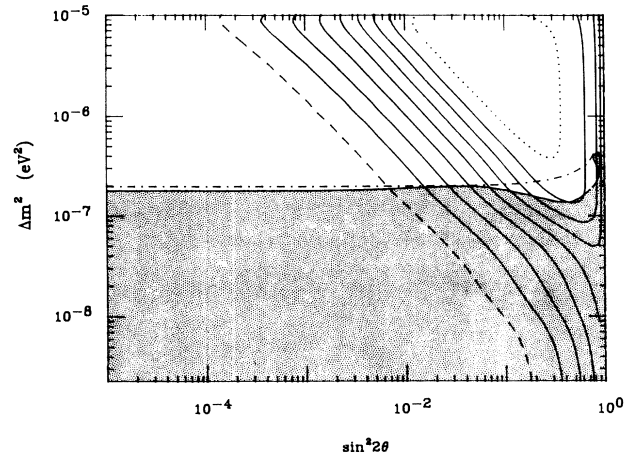


FIG. 12. The comparison of the survival probabilities for the CI detector in the quiet and active Sun. The contours are the survival probabilities for the quiet Sun ($B=0$) and the shaded area represents the region where a reduction of 50% or more can be achieved in the active Sun. In the active Sun the magnetic field is the same as that of Fig. 11, but with a maximum value of 2×10^5 G. The region below the dotted-dashed line corresponds to the situation where the location of the $\nu_e \rightarrow \bar{\nu}_\mu$ resonance is outside $0.7R_\odot$.

netic moments and pointed out a possible explanation of the variation of the solar-neutrino flux with the solar cycle. This solution requires a magnetic field in the bottom of the convective zone of the Sun with $B \sim 1-2 \times 10^5$ G and a transition magnetic moment of $5-10 \times 10^{-12} \mu_B$. Because of the existence of more restrictive bounds on the transition magnetic moments for Dirac neutrinos, this solution seems to favor the possibility that the neutrinos are Majorana particles. In our discussions, following Sofia *et al.*, we assumed that the deviation from the standard solar model is perturbative. In order to assess the validity of our conclusions, it would be desirable to do a Monte Carlo study incorporating all possible variations in the solar model, very similar in spirit to the study of Bahcall and Haxton⁴¹ for the MSW effect. Unfortunately, since we do not have a simple algorithm, similar to the finite Landau-Zener approximation used by those authors, for solving the neutrino propagation problem, such a Monte Carlo study is, at present, not numerically feasible.

ACKNOWLEDGMENTS

We thank S. Sofia, S. Pakvasa, and A. Baltz for useful discussions. This research was supported in part by the University of Wisconsin Research Committee with funds granted by the Wisconsin Alumni Research Foundation, in part by National Science Foundation Grant No. PHY-8814329. The research of A.B.B. was also supported in part by the Presidential Young Investigator Program administered by the U.S. National Science Foundation.

- ¹R. Davis, D. S. Harmer, and K. C. Hoffmann, *Phys. Rev. Lett.* **20**, 1205 (1968); J. K. Rowley, B. T. Cleveland, and R. Davis, *Solar Neutrinos and Neutrino Astronomy*, proceedings of a Conference, edited by M. L. Cherry, K. Lande, and W. A. Fowler (AIP Conf. Proc. No. 126) (AIP, New York, 1985), p. 1.
- ²J. N. Bahcall, W. F. Huebner, S. H. Lubow, P. D. Parker, and R. K. Ulrich, *Rev. Mod. Phys.* **54**, 767 (1982).
- ³L. Wolfenstein, *Phys. Rev. D* **17**, 2369 (1978); **20**, 2634 (1979).
- ⁴S. P. Mikheyev and A. Yu. Smirnov, *Nuovo Cimento* **9C**, 17 (1986); *Yad. Fiz.* **42**, 1441 (1985) [*Sov. J. Nucl. Phys.* **42**, 913 (1985)].
- ⁵H. A. Bethe, *Phys. Rev. Lett.* **56**, 1305 (1986); S. P. Rosen and J. M. Gelb, *Phys. Rev. D* **34**, 969 (1986); E. W. Kolb, M. S. Turner, and T. P. Walker, *Phys. Lett. B* **175**, 478 (1986); W. C. Haxton, *Phys. Rev. Lett.* **57**, 1271 (1986); *Phys. Rev. D* **35**, 2352 (1987); V. Barger, K. Whisnant, S. Pakvasa, and R. J. N. Phillips, *ibid.* **22**, 2718 (1980); V. Barger, R. J. N. Phillips, and K. Whisnant, *ibid.* **34**, 980 (1986); S. J. Parke, *Phys. Rev. Lett.* **57**, 1275 (1986); T. K. Kuo and J. Pantaleone, *Phys. Rev. D* **35**, 3432 (1987); C. W. Kim, S. Nussinov, and W. K. Sze, *Phys. Lett. B* **184**, 403 (1987); A. Dar, A. Mann, Y. Melina, and D. Zajfman, *Phys. Rev. D* **35**, 3607 (1987); A. J. Baltz and J. Weneser, *ibid.* **37**, 3364 (1988); T. K. Kuo and J. Pantaleone, *Rev. Mod. Phys.* **61**, 937 (1989).
- ⁶A. B. Balantekin, S. H. Fricke, and P. J. Hatchell, *Phys. Rev. D* **38**, 935 (1988).
- ⁷A. Cisneros, *Astrophys. Space Sci.* **10**, 87 (1970).
- ⁸G. A. Bazilevskaya, Yu. I. Stozhkov, and T. N. Charachyan, *Pis'ma Zh. Eksp. Teor. Fiz.* **35**, 273 (1982) [*JETP Lett.* **35**, 341 (1982)]; R. Davis, in *Proceedings of the Seventh Workshop on Grand Unification*, Toyama, Japan, 1986, edited by J. Arafune (World Scientific, Singapore, 1987), p. 237.
- ⁹L. B. Okun, M. B. Voloshin, and M. I. Vysotsky, *Yad. Fiz.* **44**, 677 (1986) [*Sov. J. Nucl. Phys.* **44**, 440 (1986)].
- ¹⁰E. Kh. Akhmedov, *Phys. Lett. B* **213**, 64 (1988); E. Kh. Akhmedov and M. Yu. Khlopov, *Mod. Phys. Lett. A* **3**, 451 (1988).
- ¹¹R. Barbieri and G. Fiorentini, *Nucl. Phys.* **B304**, 909 (1988).
- ¹²H. A. Bethe, *Phys. Rev. Lett.* **63**, 837 (1989).
- ¹³C.-S. Lim and W. J. Marciano, *Phys. Rev. D* **37**, 1368 (1988).
- ¹⁴H. Minakata and H. Nunokawa, *Phys. Rev. Lett.* **63**, 121 (1989).
- ¹⁵I. Iben, Jr., *Ann. Phys. (N.Y.)* **54**, 169 (1969); Z. Abraham and I. Iben, Jr., *Astrophys. J.* **170**, 157 (1971); J. N. Bahcall and R. K. Ulrich, *ibid.* **170**, 593 (1971); S. Chitre, D. Ezer, and R. Stothers, *Astrophys. Lett.* **14**, 37 (1973); D. Bartenwerfer, *Astron. Astrophys.* **25**, 455 (1973).
- ¹⁶J. N. Bahcall, *Neutrino Astrophysics* (Cambridge University Press, Cambridge, England, 1989).
- ¹⁷R. K. Ulrich, *Astrophys. J.* **188**, 369 (1974); E. Parker, *ibid.* **175**, 261 (1971).
- ¹⁸T. M. Brown and C. A. Murrow, *Astrophys. J. Lett.* **314**, L21 (1987).
- ¹⁹H. Zirin, *Astrophysics of the Sun* (Cambridge University Press, Cambridge, England, 1988).
- ²⁰E. Schatzman and E. Ribes, in *Proceedings of the Seventh Moriond Workshop*, edited by O. Fackler and J. Tran Than Van (Editions Frontières, Gif-sur-Yvette, 1987), p. 367; E. Ribes, P. Mein, and A. Mangeney, *Nature (London)* **318**, 170 (1985).
- ²¹A. S. Endal, S. Sofia, and L. W. Twigg, *Astrophys. J.* **290**, 748 (1985).
- ²²A. J. Baltz and J. Weneser, *Nucl. Phys.* **A505**, 67 (1989).
- ²³B. W. Lee and R. E. Shrock, *Phys. Rev. D* **16**, 1444 (1977); W. Marciano and A. Sanda, *Phys. Lett.* **67B**, 303 (1977); M. A. B. Beg, W. J. Marciano, and M. Ruderman, *Phys. Rev. D* **17**, 1395 (1977); K. Fujikawa and R. E. Shrock, *Phys. Rev. Lett.* **45**, 963 (1980); B. W. Lynn, *Phys. Rev. D* **23**, 2151 (1981).
- ²⁴J. E. Kim, *Phys. Rev. D* **14**, 3000 (1986).
- ²⁵M. Fukugita and T. Yanagida, *Phys. Rev. Lett.* **58**, 1807 (1987); K. S. Babu and V. S. Mathur, *Phys. Lett. B* **196**, 218 (1987).
- ²⁶H. P. Nilles, *Phys. Rep.* **110**, 1 (1984); H. Haber and G. Kane, *ibid.* **117**, 75 (1985).
- ²⁷A. Masiero, D. V. Nanopoulos, and A. Sanda, *Phys. Rev. Lett.* **57**, 663 (1986); J. L. Hewett and T. Rizzo, *Phys. Rep.* **183**, 193 (1989).
- ²⁸B. Kayser, *Commun. Nucl. Part. Phys.* **14**, 69 (1985).
- ²⁹W. J. Marciano and Z. Parsa, *Annu. Rev. Nucl. Part. Sci.* **36**, 171 (1986).
- ³⁰J. Bernstein, M. Ruderman, and G. Feinberg, *Phys. Rev.* **132**, 1227 (1963).
- ³¹J. M. Lattimer and J. Cooperstein, *Phys. Rev. Lett.* **61**, 23 (1988).
- ³²R. Barbieri and R. N. Mohapatra, *Phys. Rev. Lett.* **61**, 27 (1988).
- ³³D. Nötzold, *Phys. Rev. D* **38**, 1658 (1988).
- ³⁴M. B. Voloshin, *Pis'ma Zh. Eksp. Teor. Fiz.* **47**, 421 (1988) [*JETP Lett.* **47**, 501 (1988)]; *Phys. Lett. B* **209**, 360 (1988).
- ³⁵J. A. Morgan, *Phys. Lett.* **102B**, 247 (1981); M. Fukugita and S. Yazaki, *Phys. Rev. D* **36**, 3817 (1987).
- ³⁶P. Vogel and J. Engel, *Phys. Rev. D* **39**, 3378 (1989).
- ³⁷M. Leurer and J. Liu, *Phys. Lett. B* **219**, 304 (1989); F. Giuliani and S. Ranfone, *Nucl. Phys.* **B325**, 724 (1989).
- ³⁸R. S. Raghavan, S. Pakvasa, and B. A. Brown, *Phys. Rev. Lett.* **57**, 1801 (1986); R. S. Raghavan and S. Pakvasa, *Phys. Rev. D* **37**, 849 (1988).
- ³⁹A. B. Balantekin, F. Loreti, S. Pakvasa, and R. S. Raghavan (in preparation).
- ⁴⁰S. Sofia (private communication).
- ⁴¹J. N. Bahcall and W. C. Haxton, *Phys. Rev. D* **40**, 931 (1989).

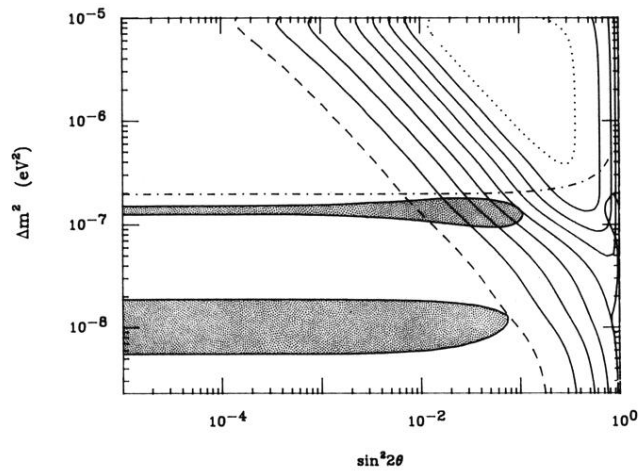


FIG. 11. The comparison of the survival probabilities for the Cl detector in the quiet and active Sun. The contours are the survival probabilities for the quiet Sun ($B=0$) and the shaded area represents the region where a reduction of 40% or more can be achieved in the active Sun. In the active Sun the magnetic field is confined to the convective zone as calculated by Endal, Sofia, and Twigg (Ref. 21) (with a maximum value of 10^5 G). The transition magnetic moment is taken to be $10^{-11} \mu_B$. The region below the dotted-dashed line corresponds to the situation where the location of the $\nu_e \rightarrow \bar{\nu}_\mu$ resonance is outside $0.7R_\odot$.

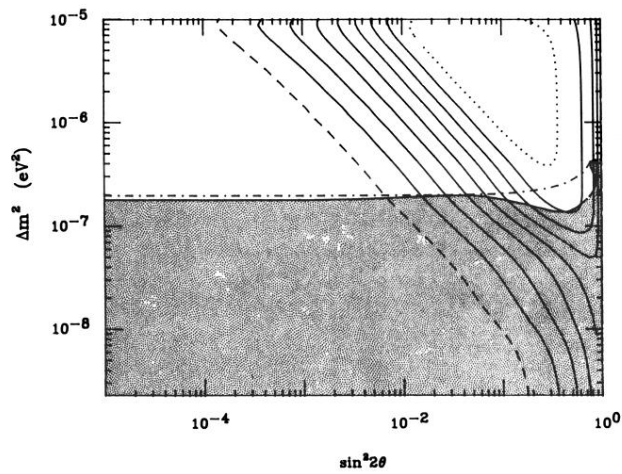


FIG. 12. The comparison of the survival probabilities for the Cl detector in the quiet and active Sun. The contours are the survival probabilities for the quiet Sun ($B=0$) and the shaded area represents the region where a reduction of 50% or more can be achieved in the active Sun. In the active Sun the magnetic field is the same as that of Fig. 11, but with a maximum value of 2×10^5 G. The region below the dotted-dashed line corresponds to the situation where the location of the $\nu_e \rightarrow \bar{\nu}_\mu$ resonance is outside $0.7R_\odot$.